# A quartz-enhanced photoacoustic sensor for H2S trace-gas detection at 2.6 μm

**ARTICLE** *in* APPLIED PHYSICS B · DECEMBER 2014

Impact Factor: 1.86 · DOI: 10.1007/s00340-014-5991-y

Appl. Phys. B
DOI 10.1007/s00340-014-5991-y

**Applied Physics B**
**Lasers and Optics**

# A quartz-enhanced photoacoustic sensor for $H_2S$ trace-gas detection at 2.6 μm

**S. Viciani · M. Siciliani de Cumis · S. Borri · P. Patimisco · A. Sampaolo · G. Scamarcio · P. De Natale · F. D'Amato · V. Spagnolo**

Received: 29 October 2014 / Accepted: 16 December 2014


**Abstract** We report on the realization of a quartz-enhanced photoacoustic (QEPAS) sensor for measurement of $H_2S$ gas traces. A distributed feedback diode laser working at 2.64 μm wavelength has been coupled to an acoustic detection module composed of a quartz tuning fork and a micro-resonator system, and the QEPAS signal has been optimized in terms of gas sample pressure and laser frequency modulation depth. The sensor shows a very good linearity with respect to the $H_2S$ concentration. We performed an Allan–Werle variance analysis to investigate the sensor long-term stability, and we reached a detection limit of four parts per million for 1-s integration time and 500 parts per billion in 60-s integration time. The realized QEPAS sensor represents a good compromise between performance and handiness, in view of a fully portable device.

## 1 Introduction

Gas detection has a great impact across a wide range of applications. Highly sensitive trace-gas sensors are employed to ensure safety in industrial environments, where monitoring of key species in products and processes is required (toxic or flammable gases, for example) [1]. The use of gas detectors is also widespread in atmospheric science, where they are used to measure and understand the profile and pathways of different gas species with particular attention to greenhouse gases [2]. Medical applications include the study of various potential biomarker gases for use, e.g., in breath diagnostics, including nitric oxide (NO) [3], ethane, ammonia ($NH_3$) [4], and many other gases [5].

Gas sensors based on optical absorption have the advantage of fast response time (time constants below 1 s are feasible), minimal drift, and high gas selectivity, with zero cross-response to other gases as long as the absorption feature is carefully selected. Measurements can be performed in real time and in situ, and this is of crucial importance for industrial process control and environmental applications. In terms of cheapness, optical gas sensing fills an important gap between low cost sensors with limited performance and high-end laboratory equipment, which can presently measure concentrations well below one parts per trillion (ppt) [6]. Among optical gas sensing techniques, quartz-enhanced photoacoustic spectroscopy (QEPAS) is one of the most compact and robust methods for trace-gas detection. QEPAS is an alternative approach to standard photoacoustic detection of trace gases employing a quartz tuning fork (QTF) as a sharply resonant acoustic transducer to detect weak photoacoustic excitation induced by a modulated laser source absorbed by the gas target and allowing the use of extremely small volumes [7]. Very efficient QCL-based QEPAS sensors have been demonstrated for trace detection of several chemical species, such as $NH_3$, NO, $CO_2$, $N_2O$, CO, $CH_2O$ [7], and a record detection limit of 50 ppt concentration on $SF_6$ has been reported [8]. One of the most challenging gases whose detection finds applications in all the fields mentioned above is hydrogen sulfide ($H_2S$). It can be found in petroleum, natural gas (up to 90 %), volcanoes, and well water (often because of the

S. Viciani · M. Siciliani de Cumis · S. Borri (✉) · P. De Natale · F. D'Amato
CNR, Istituto Nazionale di Ottica (INO), European Laboratory for Nonlinear Spectroscopy (LENS), Via Carrara 1, 50019 Sesto Fiorentino, FI, Italy
e-mail: simone.borri@ino.it

P. Patimisco · A. Sampaolo · G. Scamarcio · V. Spagnolo
Dipartimento Interateneo di Fisica, CNR, Istituto di Fotonica e Nanotecnologie (IFN) UOS Bari, Università e Politecnico di Bari, Via Amendola 173, 70126 Bari, BA, Italy

Published online: 30 December 2014

activity of sulfate-reducing bacteria) [9]. About 10 % of the total emissions of $H_2S$ are due to human activity. By far, petroleum plants produce the largest amounts of $H_2S$. Other sources of $H_2S$ include coke ovens, paper mills, and tanneries. $H_2S$ is produced when elemental sulfur is exposed to organic material, especially at high temperatures. This gas is also present in the field of renewable energies. In geothermal power plants, monitoring of underground gas emission becomes very important in order to protect both people working there and people living in proximity of geothermal installations. Recently, the interest toward $H_2S$ has been driven also by human pathologies such as bacterial overgrowth of the small intestine [10].

High-sensitivity in-field detection of $H_2S$ is challenging for many aspects, in particular for its aggressiveness and toxicity. The concentration limits set by the US Occupational Safe and Health Administration (OSHA) is 20 ppm for long lasting exposure, and a peak limit of 50 ppm for no longer than 10 min, if no other measurable exposure occurs [11]. Exposure to 100 ppm of $H_2S$ leads to the loss of sense of smell in a few minutes. Inhalation of concentrations of 500–1,000 ppm will cause quickly unconsciousness and death through respiratory paralysis and asphyxiation. Real time in situ monitoring of $H_2S$ becomes essential in order to protect both people working in industrial sites, which have $H_2S$ as secondary product, and people living in proximity. Moreover, with its typical bad smell of rotten eggs, this gas turns out to be very unpleasant even in safe concentrations (our nose is sensible to much less than 0.1 ppm).

Many techniques have been used for $H_2S$ detection. The most common are indirect measurements needing calibration operations: detector tubes [12] indicate the amount of gas by a color change of chemically coated granules in a glass tube, and electrochemical monitors must be calibrated with a known gas concentration. These techniques are reliable for high concentrations. For small concentrations detection (the most common target of commercial products), instruments based on the conversion of $H_2S$ to $SO_2$ are mostly used (for instance, Thermo Environmental $SO_2/H_2S$ analyzer, model 450i). In these sensor systems, $SO_2$ is detected by using UV fluorescence, and $H_2S$ concentration is calculated by using the chemical conversion efficiency from $H_2S$ to $SO_2$. A compact, rugged, and portable fiber-optic evanescent-field laser sensor and uncoated fused-silica multi-mode fiber with a single-mode DFB laser diode operating around 1.57 μm were developed for $H_2S$ detection in the gas streams of volcanic fumaroles, providing a detection limit of 100 ppm [13]. $H_2S$ trace detection by means of a DFB diode laser-based off-axis integrated cavity output spectroscopy (OA-ICOS) led to a minimum detectable concentration of 670 ppb for a 2-s averaging time [14]. A detection limit of 500 ppb was reported with a dual-channel $H_2S$ photoacoustic sensor [15] employing

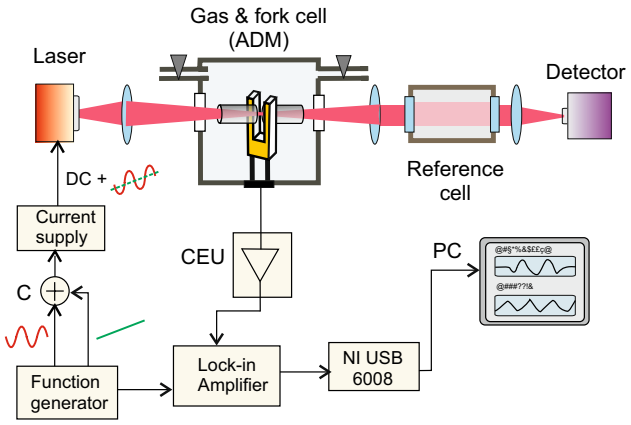


**Fig. 1** Schematic of the QEPAS sensor. *ADM* acoustic detection module; *DC* direct current; *CEU* control electronics unit; *PC* personal computer; *C* power combiner

a single-mode, fiber-coupled, room temperature, telecommunication-type diode laser at 1,574.5 nm (40 mW output optical power), and two identical resonant photoacoustic cells. In order to reach such sensitivity levels, careful calibration of the sensor and long-averaging times (~30 min) were required. With a similar telecom fiber-coupled diode laser, a QEPAS sensor providing a noise equivalent concentration of 10 ppm [16] (1-s integration time) was demonstrated. Very recently, a record detection limit of 450 ppb (3-s integration time) was reported at 7.9 μm wavelength with a QEPAS sensor based on a widely tunable fiber-coupled external-cavity quantum-cascade laser [17] with an optical power of 45 mW.

In this paper, we report on a compact, robust, and cost-effective QEPAS sensor for $H_2S$ detection based on a diode laser emitting at ~2.6 μm. With 3 mW laser power available for gas interaction, the sensor demonstrated fast $H_2S$ detection down to 4 ppm with 1-s integration time, which can be pulled down to 500 ppb for 60-s integration time. The system was tested on $H_2S$ dilutions in both dry and wet (2 % relative water concentration) nitrogen. Such measurements demonstrated a sensible influence of water vapor on the QEPAS signals, which can be quantified and taken into account for $H_2S$ in-field monitoring.

## 2 Experimental setup

A schematic of our QEPAS sensor is shown in Fig. 1. The laser source is a room temperature continuous-wave diode laser (Nanoplus, model 525-2640-2) emitting around 3,788 $cm^{-1}$ (2.64 μm), with output power up to 5 mW. The laser frequency can be finely tuned by applying a voltage ramp on the driving current by means of a modulation input port (tuning coefficient about 0.94 GHz/mA). The same port can be used for

the frequency modulation of the laser radiation up to around 1 MHz by applying a sinusoidal dither on the current driver.

The beam exiting the laser is collimated by means of a $CaF_2$ lens, subsequently focused into the acoustic detection module (ADM), housed in a vacuum-thigh cell designed for spectroscopic analysis of both static and flowing gas, and equipped with two ZnSe windows. The pressure and flow rate of the sample gas through the cell are controlled and maintained at the desired level using a pressure controller and gas flow meter (MKS Instruments Type 640). A reference cell, filled with pure $H_2S$ at 5.3 mbar, and a thermoelectrically cooled pyroelectric detector (VIGO model PVI-4TE-3.4) are placed behind the ADM housing, allowing to monitor the laser frequency scan of the selected molecular transition.

The ADM is composed of a standard QTF (300-μm prong spacing, 32.8 kHz resonance frequency) and a couple of thin metallic tubes acting as organ-pipe micro-Resonators (mR) [18], with 4-mm length and 0.6-mm internal diameter. The radiation has to be focused through the tubes and the gap between the tines in such a way that it passes through the ADM without hitting it. This is mandatory for QEPAS sensing since the radiation blocked by the ADM creates an undesirable background that is usually several times larger than the QTF thermal noise level and is accompanied by a shifting fringe-like interference pattern, which limits the detection sensitivity [19, 20]. By measuring the optical power after the ADM, we verified that the focused laser beam passed across the sensing system without hitting it. The QTF signal is processed by a transimpedance amplifier (gain factor 30) and a control electronic unit (CEU). The latter is also used to measure the electromechanical parameters of the QTF: its dynamic resistance $R$, quality factor $Q$, and resonance frequency $f_0$. The physical parameters measured for our QTF at selected working conditions (165 mbar sample pressure) using $N_2$ as gas carrier were $Q = 19{,}908$, $f_0 = 32{,}758.54$ Hz and $R = 62.6$ kΩ. From the measured resistance, we extracted a QTF thermal noise of ~2.97 μV (with 0.3335 Hz detection bandwidth) [21]. In order to retrieve the QEPAS signal, we implemented a wavelength modulation (WM) detection by applying a sinusoidal modulation to the diode laser current at half of the QTF resonance frequency $f_0/2$ and detecting the QTF response at $f_0$ (2$f$-demodulation), by means of a lock-in amplifier controlled by an USB data acquisition card (National Instruments DAQ-Card USB6008) via a LabVIEW-based software. In addition, spectral scans over the molecular absorption line were performed by tuning the laser frequency across the line by means of a linear ramp applied to the driving current.

### 2.1 Preliminary characterization

The selected $H_2S$ transition for the sensor validation is the (331–330) ro-vibrational transition at 3,788.556 wavenumber, with line strength $S = 1.67 \times 10^{-21}$ cm/molecule [22]. The QEPAS system response was preliminarily investigated for different pressures and frequency modulation depth values to determine the best operating condition in terms of highest signal-to-noise ratio. Acting on both gas pressure and modulation depth, we found the optimal QEPAS sensor response at a modulation depth of 2.1 GHz and a gas mixture pressure of 165 mbar. Figure 2 reported the QEPAS peak signal as a function of the gas pressure, measured for each pressure value under the related best modulation depth condition.

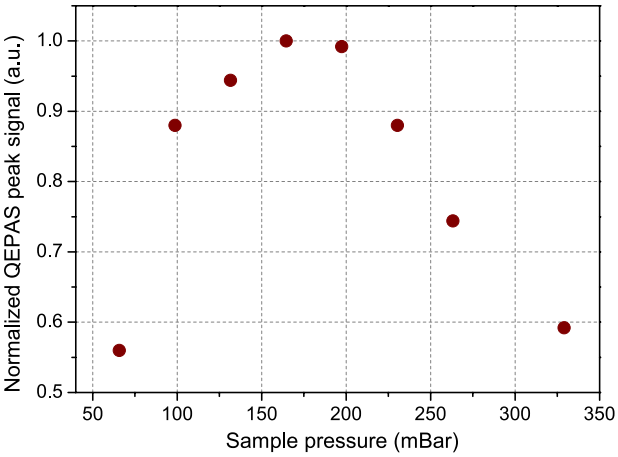


**Fig. 2** Normalized QEPAS peak signal as a function of the sample pressure. The data refer to a gas mixture composed of 500 ppm $H_2S$ in dry $N_2$, for a modulation depth of 2.1 GHz

An important issue when dealing with sensors for in-field monitoring of a specific molecule is the presence of nearby water absorption lines, which has to be taken into account for the selection of the target line. From the spectroscopic point of view, water is an interfering molecule, as it has strong absorptions through almost all the infrared spectrum, from the near-IR to the THz range. In particular, due to similarities in the molecular structure, water absorption lines are often close to $H_2S$ ones. Dealing with standard air samples (as it occurs in in-field monitoring), the typically high concentrations of water vapor (few percent) are sufficient to hide $H_2S$ absorbance or at least to interfere with it, despite sophisticated detection methods are used. Water vapor can be removed by using Nafion membrane or magnesium perchlorate filters. In these cases, water is extracted from the sample, and high-reliability $H_2S$ traces quantification is possible. Nonetheless, this means adding components to the measurement apparatus, requiring continuous maintenance and checks and so on. It is indeed more convenient, if possible, to carefully select a target line far enough from interfering water lines in order to keep the detection system as simple as possible. For our sensor, we selected a quite isolated $H_2S$ line, with

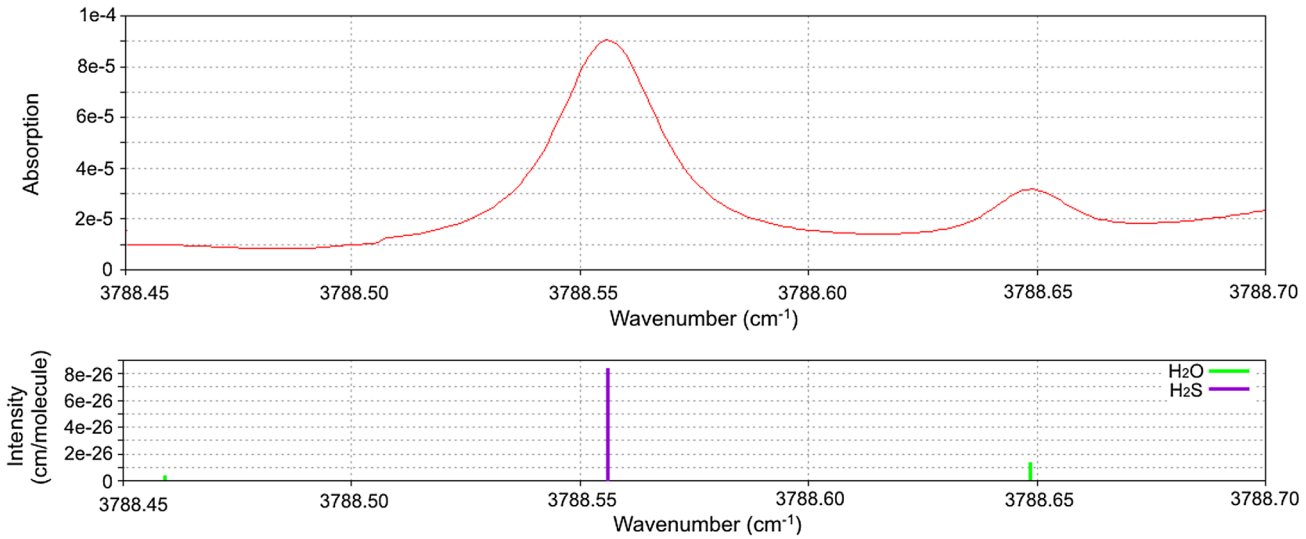


**Fig. 3** Simulated absorption spectrum of a gas mixture composed of 50 ppm of $H_2S$ in wet $N_2$ (2 % water vapor concentration). The simulation was performed at an operating pressure of 165 mbar and 300 K temperature (and a nominal absorption length of 10 cm). In the bottom graph is shown the corresponding stick spectrum of the $H_2S$ and $H_2O$ lines

only one possible interfering water line about 2.8 GHz far away. Figure 3 shows a simulation of the direct absorption spectrum of a 50 ppm $H_2S$ dilution in wet $N_2$ (2 % water vapor concentration) around the selected target line calculated at the operating pressure of 165 mbar [23]. As it can be seen, in our working pressure conditions the presence of a nearby water line does not sensibly affect the $H_2S$ absorption profile.

## 2.2 Spectroscopic measurements

The sensor has been tested with several gas mixture samples with different $H_2S$ concentrations in the range 0–500 ppm. A trace-gas standard generator is used to produce $H_2S$ concentrations in the range 0–500 ppm, using pure or humidified $N_2$ as the diluting gas, starting from a certified 500 ppm $H_2S$ in $N_2$ mixture. We use a Nafion humidifier (PermaPure) to add water vapor to the gas samples. The measured QEPAS peak values for a set of spectral acquisitions of dry $H_2S$:$N_2$ mixtures with 500-ms lock-in integration time are reported in Fig. 4. The acquired data points demonstrate the linear response of the sensor versus the $H_2S$ concentration.

Two representative QEPAS spectral scans corresponding to the same relative $H_2S$ concentration (80 ppm) at the working pressure of 165 mbar are shown in Fig. 5. The two acquisitions refer to different gas samples: spectrum in Fig. 5a refers to a $H_2S$ dilution in dry $N_2$, while in Fig. 5b wet $N_2$ (2 % water vapor concentration) was used. In both cases, the same lock-in integration time of 500 ms and 12 dB/oct filter slope was used. This comparison is required

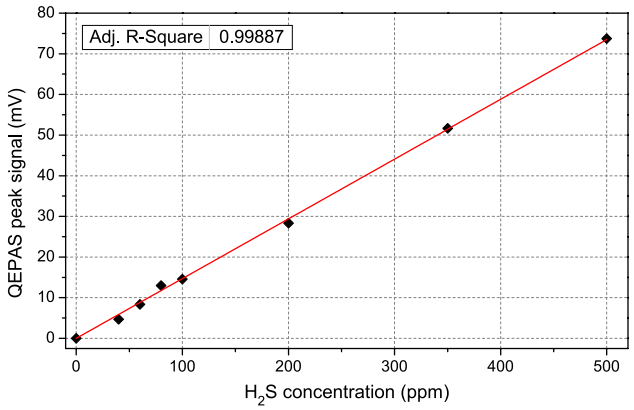


**Fig. 4** QEPAS peak signal versus $H_2S$ concentration for dry $H_2S$:$N_2$ mixtures. The *solid line* is a linear fit of the data, showing the linear behavior of the sensor

in order to check whether the QEPAS signal is affected or not by the presence of water vapor in the sample. Indeed, in the previous paragraph, we showed that the selected $H_2S$ line is far enough from possible interfering water lines. However, dealing with photoacoustic detection, water can affect the spectroscopic signal also by means of a different mechanism, i.e., by acting as promoter of vibrational-translational (VT) relaxation processes. As reported in [24], $H_2S$ shows similar vibrational de-excitation velocity compared to $H_2O$, thus the effects of $H_2O$ as a relaxation promoter for the $H_2S$:$N_2$ mixture should be almost negligible. This is indeed what was recently found for a QEPAS sensor operating in the mid-infrared range (around 8 μm), where no

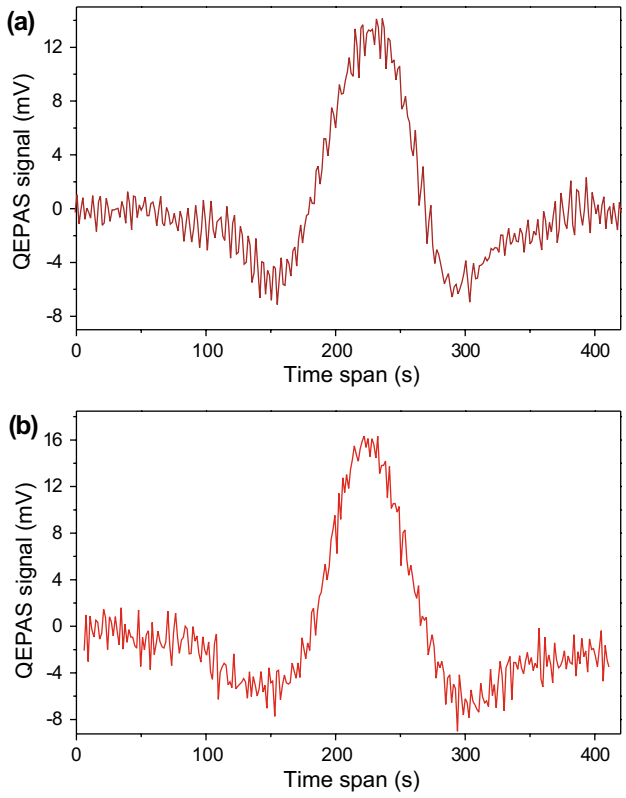


**Fig. 5** 2*f*-QEPAS spectral scans corresponding of 80 ppm $H_2S$ in dry (**a**) and wet (**b**) $N_2$ samples, as discussed in the text. Both measurements were acquired with 500-ms lock-in integration time

sensible variation of the QEPAS signal between the dry and wet cases was observed [17]. However, this cannot exclude that, when operating in different spectral regions, the situation changes due to a different distribution of the ro-vibrational levels. This is reported, for example, in Ref. [15] where a slightly different behavior between the two cases has been observed.

In our case, the spectra show a typical second-derivative shape, slightly distorted because of non-negligible residual amplitude modulation of the laser during the scan [25]. The noise level, measured as the standard deviation of the measured data points in the flat regions of the spectra, is almost the same (~1 mV rms), but the peak value of the wet dilution is about 30 % higher than that of the dry sample. We had no possibility to make a systematic analysis of the signal dependence on the $H_2O$ concentration, but indeed our result shows that the presence of water vapor has a not negligible effect on $H_2S$ QEPAS measurements at our working wavelength. This makes sensor calibration required in case of precise in-field measurements, together with simultaneous measurement of the water concentration.

Focusing on the dry sample, by analyzing the signal-to-noise ratios of the acquired spectra, we extracted a

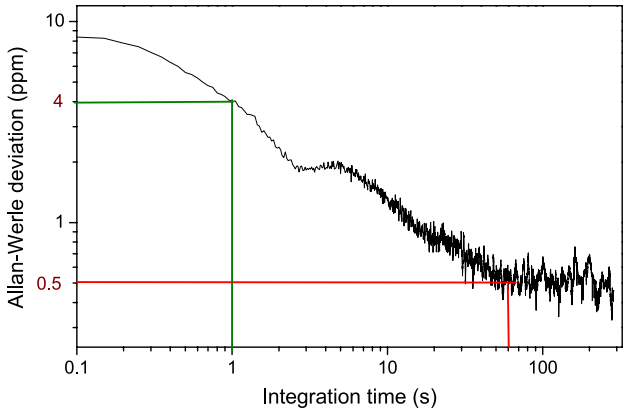


**Fig. 6** Allan–Werle deviation of the QEPAS signal as a function of the integration time. The curve has been obtained by analyzing a 70 min-long acquisition of the signal (150-ms sampling time and lock-in set to 50 ms time constant) measured for pure $N_2$ at 165 mbar pressure

minimum detectable concentration $C_{min} = 4$ ppm of $H_2S$ in dry $N_2$ for 1-s lock-in integration time. This corresponds to a noise equivalent absorption coefficient (NEAC) $\alpha_{min} = 3.4 \times 10^{-7}$ cm$^{-1}$. By taking into account the laser power available for sample interaction (~3 mW), we extract a normalized noise equivalent absorption (NNEA) of $2.4 \times 10^{-9}$ Wcm$^{-1}$Hz$^{-1/2}$, which is about one order of magnitude better than that recently measured in our group using a QEPAS sensor working at 8 μm [17] and more than two times better than the record value reported in [16].

Finally, an Allan–Werle deviation analysis of the QEPAS signal for pure $N_2$ at 165 mbar pressure was performed in order to determine the best achievable sensitivity of the sensor. The result of this analysis is reported in Fig. 6, showing that the minimum detection sensitivity can be pulled down to 500 ppb for 1-min integration time.

### 2.3 Comparison among QEPAS spectrometers for $H_2S$

The measurements in this paper have been carried out in an intermediate spectral region as compared to the two measurements already available in literature. A detailed comparison among the three different spectrometers is shown in Table 1.

It is evident that the best performance can be obtained in the mid-infrared, where the detection limit is lower, and the effect of water is negligible, but at the expenses of dimensions, weight, and cost. At higher frequencies, the performance are slightly reduced in terms of detection limit, but the analyzers take advantage of size and cost of the laser sources for the realization of portable devices for in-field applications. For both the near-IR sensors, a calibration vs water content is required. The cost of a laser source at

**Table 1** Comparison of the sensitivity results on $H_2S$ detection between this QEPAS sensor and those previously reported in literature

| | Near-IR [16] | Near-IR [this paper] | Mid-IR [17] |
|---|---|---|---|
| Frequency ($cm^{-1}$) | 6,320.61 | 3,788.56 | 1,266.93 |
| Laser power (mW) | 38.3 | 3 | 45 |
| Line strength (cm/molecule) | $1.06 \times 10^{-22}$ | $1.67 \cdot 10^{-21}$ | $1.51 \times 10^{-21}$ |
| Detection limit (ppm) @ 1 s integration time in dry sample | 10.1 | 4 | 1.3 |
| NEAC ($cm^{-1}$) | $1.4 \times 10^{-7}$ | $3.4 \times 10^{-7}$ | $1.0 \times 10^{-7}$ |
| NNEA ($cm^{-1} \times W/\sqrt{Hz}$) | $5.8 \times 10^{-9}$ | $2.4 \times 10^{-9}$ | $2.1 \times 10^{-8}$ |
| Detection limit for longer integration time | Not available | 500 ppb @ 60 s | 330 ppb @ 30 s |
| Water interference | About 10 % with 1.1–1.4 % $H_2O$ concentration | About 30 % with 2 % $H_2O$ concentration | Negligible |
| Laser package | Butterfly | TO5 | L 16 cm × W 8.5 cm × H 8.5 cm + chiller |
| Laser cost (k€), approx. | Not available | 7.5 | 43 |

3,800 $cm^{-1}$ is surely higher than in the near infrared, but the features of the analyzer are quite better, despite the lower laser power. Our near-IR sensor appears to be an optimal compromise between detection limit and handiness, although a precise calibration of water vapor effects is mandatory.

## 3 Conclusions

In conclusion, a QEPAS sensor operating at 2.6 μm for $H_2S$ trace-gas detection has been reported. With 3 mW of laser power available for gas interaction, the apparatus demonstrated a fast (1-s integration time) detection sensitivity down to 4 ppm, which is reduced to 500 ppb for 1 min integration. In order to make possible in-field measurements, the sensor was designed to interrogate a $H_2S$ transition, which is not sensibly affected by nearby interfering water lines. Nonetheless, preliminarily measurements showed a sensible effect of water vapor as V-T relaxation promoter, leading to the necessity of a proper sensor calibration for monitoring wet $H_2S$ samples. The compactness, the practicality, and the cheapness of our sensor, along with the possibility of remote control, low power consumption, and automatic operation, could lead to the realization of a low cost network of environmental monitoring stations for $H_2S$ detection, e.g., in volcanic or geothermal areas.

**Acknowledgments** The authors gratefully acknowledge the financial support from the Italian Ministry of University and Research (MIUR) through the project "Active Ageing at Home" (CTN01_00128_297061, Area TAV - Tecnologie per gli Ambienti di Vita), from Regione Toscana within the frame of POR CReO FESR 2007–2013, Project SIMPAS (Innovative Measurement Systems for the Protection of Environment and Health), and the Italian research projects PON01 02238, PON02 00675 and PON02 00576.

## References

1. M. Lackner, Rev. Chem. Eng. **23**, 65 (2007)
2. P. Werle, F. D'Amato, S. Viciani, in *Lasers in Chemistry: Probing and Influencing Matter*, vol 1, chapter 9, (Wiley-VCH, Weinheim, 2008), p. 255. ISBN 978-3-527-31997-8
3. V. Spagnolo, R. Lewicki, L. Dong, F. K. Tittel, in *Proceeding of the IEEE International Symposium on Medical Measurements and Applications MeMeA2011*, p. 332 (2011). doi:10.1109/MeMeA.2011.5966773
4. F.K. Tittel, R. Lewicki, L. Dong, K. Liu, T.H. Risby, S. Solga, T. Schwartz, in *Proc. SPIE 8223, Photons Plus Ultrasound: Imaging and Sensing 2012*, *82230E* (23 February 2012). doi: 10.1117/12.912273
5. D. Smith, P. Španěl, Analyst **132**, 390 (2007)
6. I. Galli, S. Bartalini, P. Cancio, P. De Natale, D. Mazzotti, G. Giusfredi, M.E. Fedi, P.A. Mandò, Radiocarbon **55**, 213 (2013)
7. P. Patimisco, G. Scamarcio, F.K. Tittel, V. Spagnolo, Sensors **14**, 6165 (2014)
8. V. Spagnolo, P. Patimisco, S. Borri, G. Scamarcio, B.E. Bernacki, J. Kriesel, Opt. Lett. **37**, 4461 (2012)
9. L.L. Barton, G.D. Fauque, Adv. Appl. Microbiol. **68**, 4198 (2009)
10. L. Ciaffoni, R. Peverall, G.A.D. Ritchie, J. Breath Res. **5**, 024002 (2011)
11. U.S. Occupational Safe and Health Administration (OSHA). https://www.osha.gov/
12. J. Patterson, M.G. Mellon, Anal. Chem. **24**, 1586 (1952)
13. U. Willer, D. Scheel, I. Kostjucenko, C. Bohling, W. Schade, E. Faber, Spectrochim. Acta A **58**, 2427 (2002)
14. W. Chen, A.A. Kosterev, F.K. Tittel, X. Gao, W. Zhao, Appl. Phys. B **90**, 311 (2008)
15. A. Varga, Z. Bozóki, M. Szakáll, G. Szabó, Appl. Phys. B **85**, 315 (2006)
16. A.A. Kosterev, L. Dong, D. Thomazy, F.K. Tittel, S. Overby, Appl. Phys. B **101**, 649 (2010)
17. M. Siciliani de Cumis, S. Viciani, S. Borri, P. Patimisco, A. Sampaolo, G. Scamarcio, P. De Natale, F. D'Amato, V. Spagnolo, Opt. Express **22**, 28222 (2014)
18. H. Wu, L. Dong, W. Ren, W. Yin, W. Ma, L. Zhang, S. Jia, F.K. Tittel, Sens. Actuators B **206**, 364 (2015)
19. V. Spagnolo, A.A. Kosterev, L. Dong, R. Lewicki, F.K. Tittel, Appl. Phys. B **100**, 125 (2010)

20. L. Dong, V. Spagnolo, R. Lewicki, F.K. Tittel, Opt. Express **19**, 24037 (2011)
21. A.A. Kosterev, F.K. Tittel, D.V. Serebryakov, A.L. Malinovsky, I.V. Morozov, Rev. Sci. Instrum. **76**, 043105 (2005)
22. L.S. Rothman, I.E. Gordon, Y. Babikov, A. Barbe, D. Chris Benner, P.F. Bernath, M. Birk, L. Bizzocchi, V. Boudon, L.R. Brown, A. Campargue, K. Chance, E.A. Cohen, L.H. Coudert, V.M. Devi, B.J. Drouin, A. Fayt, J.M. Flaud, R.R. Gamache, J.J. Harrison, J.M. Hartmann, C. Hill, J.T. Hodges, D. Jacquemart, A. Jolly, J. Lamouroux, R.J. Le Roy, G. Li, D.A. Long, O.M. Lyulin, C.J. Mackie, S.T. Massie, S. Mikhailenko, H.S.P. Müller, O.V. Naumenko, A.V. Nikitin, J. Orphal, V. Perevalov, A. Perrin, E.R. Polovtseva, C. Richard, M.A.H. Smith, E. Starikova, K. Sung, S. Tashkun, J. Tennyson, G.C. Toon, V.G. Tyuterev, G. Wagner, J. Quant. Spectrosc. Radiat. Transf. **130**, 4–50 (2013)
23. Simulation from *spectra.iao.ru*
24. H.-J. Bauer, A.C.C. Paphitis, R. Schotter, Physica **47**, 109 (1970)
25. P. Patimisco, S. Borri, A. Sampaolo, H.E. Beere, D.A. Ritchie, M.S. Vitiello, G. Scamarcio, V. Spagnolo, Analyst **139**, 2079 (2014)